

Atomic-scale manipulation of potential barriers at SrTiO₃ grain boundaries

Pradyumna Prabhumirashi and Vinayak P. Dravid^{a)}

Department of Materials Science and Engineering, Northwestern University, Evanston, Illinois 60208

Andrew R. Lupini, Matthew F. Chisholm, and Stephen J. Pennycook

Condensed Matter Sciences Division, Oak Ridge National Laboratory, Oak Ridge, Tennessee 37831

(Received 9 May 2005; accepted 26 July 2005; published online 16 September 2005)

In oxide grain boundaries (GBs), oxygen ions and their vacancies serve as a common denominator in controlling properties such as GB barrier height and capacitance. Therefore, it is critical to analyze, control and manipulate oxygen and vacancies at oxide interfaces as most of the practical devices are almost always influenced by the presence of electrostatic potential barriers at interfaces. Here, we report adjustment of a single GB potential barrier via manipulation of oxygen vacancy concentration using simple oxidation and reduction treatments. We validate our analysis with aberration-corrected HAADF imaging and column-by-column EELS coupled with macroscopic transport measurements of isolated GBs to gain important insight into the physical attributes of GB potential barriers. © 2005 American Institute of Physics. [DOI: 10.1063/1.2046734]

It is well-known that oxygen ions and their vacancies serve as a common denominator in oxides for controlling their technologically important properties.^{1,2} Recent reports^{3,4} have elegantly demonstrated the ability to control, manipulate and analyze oxygen and vacancies at the nanoscale, albeit in the bulk crystals. However, in addition to control of the bulk structure and stoichiometry, it is equally important to atomically “engineer” interfaces in oxide systems because almost all practical devices are greatly influenced by the presence of electrically active interfaces. In fact, the trapping and flow of mobile charge carriers across and at interfaces form the basis for numerous electronic, transport, and capacitive properties of interfacial systems in oxides. Thus, the key to understand, manipulate and realize the full functionality of oxides is to engineer oxygen and vacancy content at individual interfaces by suitable doping and heat treatment procedures. Although the utility and study of GB doping has an extensive history,^{6–8} only few reports exist on structure-property co-relationship of single SrTiO₃ GBs.^{5,9–11}

We oriented bicrystals of SrTiO₃ as a model system. The bicrystals are used in order to avoid the issue of geometric randomness in polycrystalline materials. Bulk donor (Nb) doped SrTiO₃ bicrystals exhibit nonlinear *I-V* behavior with resistivity almost 4 orders of magnitude higher than their single crystal counterparts.⁵ This behavior can be significantly changed by simple thermal oxidation and reduction treatments, which alter the electrostatic potential barriers at the GBs, owing to change in oxygen and vacancy content and configuration. In this letter, we investigate the effects of oxygen and oxygen vacancy concentration on the GB potential barrier.

Symmetrical tilt bicrystals of SrTiO₃, 24° [001], were obtained from CrysTec GmbH (Berlin, Germany). In order to manipulate the oxygen vacancy concentration at the GB, one set of samples was reduced [at 800 °C with a constant flow of CO–CO₂ (5% CO by volume) for 30 min], while another set was oxidized (at 1000 °C with a constant flow of high-purity oxygen for 2 h). These were chosen simply as two diverse conditions in order to get different oxygen vacancy

concentration at the GB. Self-supporting TEM specimens were prepared using standard TEM specimen preparation techniques. The electrical characterization was carried out using a computer interface controlled current source and a multimeter.¹² The detailed atomic structure of the GB, including local chemistry and valence changes were studied using scanning transmission electron microscope (STEM) equipped with a spherical aberration (*C_s*) corrector (Nion Co., Kirkland WA, USA).¹³ *C_s* corrected STEM offers unprecedented opportunity to probe the details of atomic structure at grain boundaries with a sub-Å electron probe^{14,15} using high angle annular dark field (HAADF) or so-called Z-contrast and phase contrast bright-field (BF) STEM imaging, coupled with atomic-scale electron energy loss spectroscopy (EELS). The electrons form the HAADF image in which the intensity of each atomic column, to a good approximation, is directly proportional to the atomic number $\sim Z^2$.¹⁶ For this study, HAADF imaging was performed using a *C_s* corrected STEM with a probe size close to 0.6 Å (VG HB603 U),¹⁴ while HAADF imaging with EELS was done using a *C_s* corrected STEM with a probe size close to 1 Å (VG HB501 UX).

Four probe dc *I-V* measurements were carried out on pristine, reduced, and oxidized SrTiO₃ bicrystals (Fig. 1). As shown in the figure, a strong nonlinear characteristic is observed, clearly marking the critical voltage (*V_C*) above which the current abruptly begins to flow. The *V_C* varies considerably with the processing conditions: ~ 0.12 V for the reduced sample, ~ 0.24 V for the pristine sample, and ~ 0.7 V for the oxidized sample. The decrease in the *V_C* for the reduced sample may be due to the decrease in the number of trap states at the GB or an increase in the number of majority charge carriers (electrons), while the increased *V_C* for the oxidized sample may be due to an increased number of traps at the GB. By looking at *V_C*, together with prebreakdown resistance (see inset of Fig. 1) it can be inferred that as compared to the pristine samples, reduced samples showed a decrease in the GB barrier height, while oxidized samples showed an increase in the GB barrier height.¹⁷

In order to probe the atomic-scale origin of this differing behavior, we imaged the reduced and oxidized 24° symmet-

^{a)}Electronic mail: v-dravid@northwestern.edu

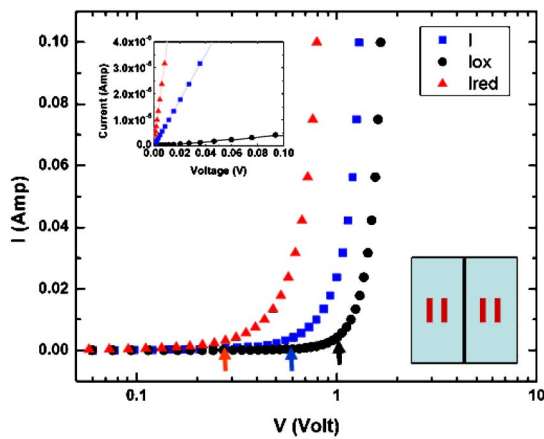


FIG. 1. (Color online) 4 probe dc I - V measurements (plotted on a semilog scale) across the GB in as-received (■, legend I), oxidized (●, legend lox), and reduced (▲, legend lred) SrTiO₃. The top inset shows prebreakdown I - V characteristic with a linear fit. Note that while reduction leads to a decrease in the prebreakdown resistance (R) and V_C (marked by arrows of respective colors), oxidation leads to an increase in the prebreakdown resistance and V_C . This change is directly related to change in the barrier height. A first order estimate of GB barrier height (ϕ) is given by the onset of the nonlinear regime in the I - V measurements. It can be seen that V_C^{pristine} is ~ 0.24 eV with $R^{\text{pristine}} \sim 1.139 \times 10^3 \Omega (\pm 2.29 \Omega)$, while V_C^{reduced} is ~ 0.12 eV with $R^{\text{reduced}} \sim 263.85 \Omega (\pm 1.24 \Omega)$ and V_C^{oxidized} is ~ 0.7 eV with $R^{\text{oxidized}} \sim 2.397 \times 10^4 \Omega (\pm 310.7 \Omega)$. The bottom inset shows a schematic of measurement setup (Ref. 12).

ric tilt GBs using HAADF imaging (Fig. 2). The Sr atomic columns appear brightest owing to higher atomic number of Sr compared to Ti or O. A unique GB core unit was observed in the reduced SrTiO₃ sample [Fig. 2(a)]. This unit consists

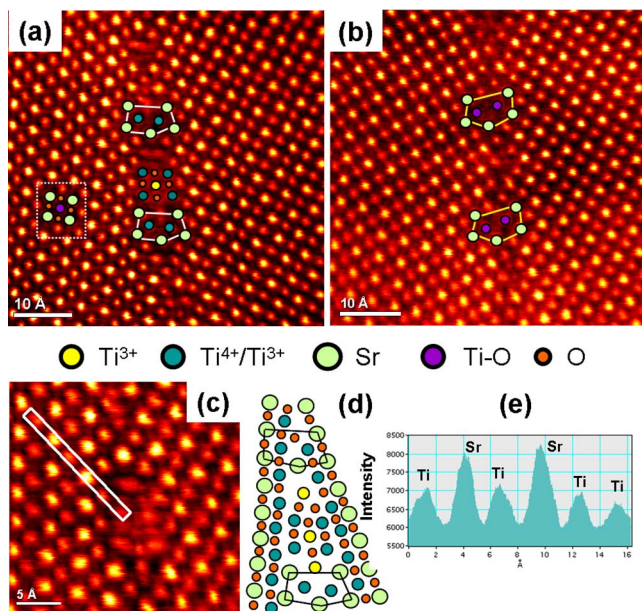


FIG. 2. (Color online) (a) HAADF image of the reduced GB. The dislocation core units are superimposed. At the center of the reduced boundary, a unique dislocation core unit is detected. This unit has the same periodicity as the other GB core units have. Inset shows a schematic of SrTiO₃ structure projection when viewed along [100]. (b) HAADF image of the oxidized GB showing periodic dislocation core units. (c) HAADF image of the reduced dislocation core unit. (d) A schematic of the reduced GB structure. It is observed that the Ti atoms in GB core exist as Ti³⁺ while those near the core have a mixed Ti³⁺/Ti⁴⁺ oxidation state, as confirmed by EEL line scans [Fig. 3(a)]. Oxygen atom positions are indicated. (e) Intensity profile along Ti-TiO-Sr-TiO [white box shown in Fig. 3(c)] columns indicating that the unit has Ti atoms at the corners.

of a central Ti atom surrounded by 4 other Ti atoms and oxygen atoms. It is postulated that the central Ti atom is present as a nominal Ti³⁺ while the surrounding Ti atoms are present as nominally mixed Ti³⁺/Ti⁴⁺. This structural unit was found to have the same periodicity as the other GB dislocation core units (between $\Sigma 13\{510\}$ and $\Sigma 85\{920\}$) but was not observed in the oxidized sample [Fig. 2(b)].

To verify the abovementioned postulate and to examine the chemistry and bonding on an atomic scale, we performed simultaneous EELS core-level spectroscopy. Specifically, the titanium $L_{2,3}$ and oxygen K edges were simultaneously recorded, with an energy resolution of better than 0.8 eV and a spatial resolution corresponding to the probe size of about 1 Å. Figures 3(a) and 3(c) show Ti $L_{2,3}$ edges and O K edges as the STEM probe scans directly across the GB in steps of 1 Å. The bulk Ti $L_{2,3}$ edge displays the typical crystal-field splitting of the L_2 and L_3 edges, due to spin-orbit coupling of t_{2g} and e_g molecular orbitals of Ti and O ions^{18–20} and is 2.2–2.4 eV for the octahedrally coordinated Ti and O in SrTiO₃. It was seen [Fig. 3(a)] that as the 1 Å STEM probe scanned across the reduced GB, the sharp splitting (bulk) gradually changed to a shoulderlike shape (2 Å from the GB) and then locally vanished at the GB. Reduction (and absence) of crystal field splitting necessarily implies a change in Ti–O coordination at the GB via change in the number of nearest oxygen neighbors and changes in Ti–O bond length. The broadening of the fine structural lines is also associated with the valence decrease of the Ti ions.¹⁸ The evolution of the fine structure of the Ti $L_{2,3}$ edge from bulk to the reduced GB is similar to published EELS data from TiO₂ (octahedrally coordinated Ti and O) as it is gradually reduced to Ti₂O₃ (semiconductor) and then to TiO (metal).²¹ The O K edge intensity decreased [Fig. 3(c)] at the GB, indicating local reduction in oxygen content. The reduction in peaks *a*, *b*, and *c* is caused by lattice distortion of the Ti–O bonds due to the oxygen vacancies, suggesting significant modulation of octahedral coordination in the vicinity of the GB.

For the oxidized sample however, it was observed that the Ti crystal-field splitting is maintained as the STEM probe scans across the boundary [Fig. 3(d)], suggesting no significant change in the Ti–O coordination. Figure 3(e) shows the Ti/O integrated intensity ratio plotted for the spectra in Figs. 3(a) and 3(d). For the reduced sample, it was observed that the Ti/O ratio increased by about $45 \pm 10\%$ locally at the GB, consistent with a reduction in oxygen concentration and corresponding increase in oxygen vacancy content. However, this contrasts to the oxidized sample, where the Ti/O ratio decreased by about $20 \pm 10\%$ at the GB, suggesting the presence of oxygen trap states, presumably oxygen adsorption, induced by oxidation.²²

The different electrical response of the oxidized and reduced samples can therefore be rationalized using the atomic-scale observations from the STEM line profiles. The reduction of a SrTiO₃ GB results in a high concentration of oxygen vacancies at the GB and subsequent change in local Ti–O coordination. The oxygen vacancies are expected to act as electron donors. The change in local Ti–O coordination is evident by the reduction of Ti⁴⁺ to Ti³⁺. An increase in oxygen vacancy concentration as well as the presence of Ti³⁺ [confirmed by EELS in Fig. 3(a)] at the GB core is expected to decrease the barrier height in the reduced sample as manifested by the decrease in the GB resistance (Fig. 1).

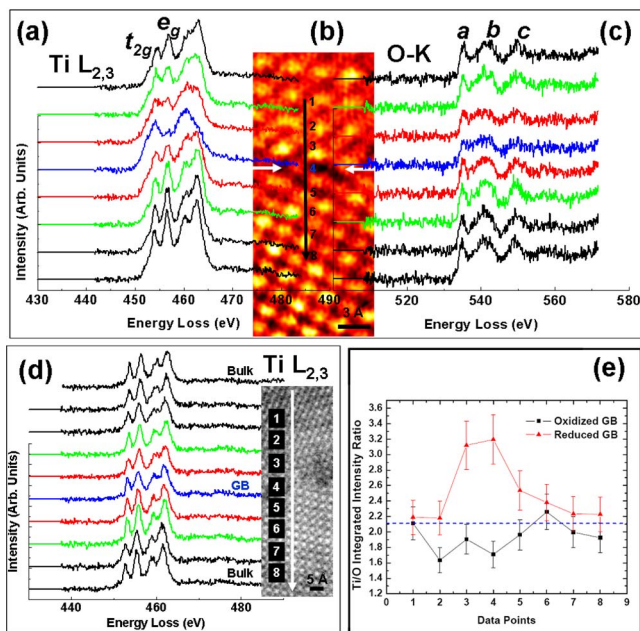


FIG. 3. (Color online) EEL spectra recorded point by point across the reduced and oxidized SrTiO₃ GBs. The spectra were taken with an acquisition time of 1 s per spectrum. The energy resolution was 0.8 eV. (a) This panel shows the background corrected Ti L_{2,3} edges for the reduced sample. The e_g - t_{2g} splitting disappears locally at the GB indicating disruption of octahedral coordination. In the GB spectrum, the Ti L_{2,3} edge onset is at a $\sim 1.1 \pm 0.8$ eV lower energy than its bulk counterpart indicating reduction of Ti⁴⁺ to Ti³⁺. (b) HAADF image shows 8 points where the respective spectrum was taken. The GB plane is indicated by white arrows. (c) This panel shows the background corrected O K edges for the reduced sample, which were collected simultaneously with Ti L_{2,3} edges. (d) Evolution of background corrected Ti L_{2,3} edges for the oxidized sample. Spectroscopy conditions were identical to those of the reduced sample. HAADF image shows the 8 points where the respective spectrum was taken. (e) Ti/O integrated intensity ratio of reduced and oxidized GBs corresponding to the 8 spectra in (a) and (d). For the reduced GB, there is a local increase in the Ti/O ratio at the GB indicating an increase in oxygen vacancy concentration. For the oxidized GB, however, there is a local decrease in the Ti/O ratio at the GB indicating a decrease in oxygen vacancy concentration. Ti/O integrated intensity ratio for bulk SrTiO₃ is shown as a dotted line. The vertical error bars reflect the 90% confidence level for Student *t*-analysis of the data.

For the oxidized sample, although no change in Ti valance was observed, the oxygen concentration at the GB was observed to increase. The increase in oxygen concentration is believed to be brought about by chemisorption of O⁻ and O²⁻ interfacial trap acceptor states. This increases the barrier height and hence increases the GB resistance as observed in electrical measurements. The oxygen chemisorption was also observed by Nakano *et al.* in the early 1990s.²² The observations are also consistent with the expected sign of the GB charge and space-charge potential proposed in electron holography experiments.^{9,23,24}

In summary, this letter reports atomic-scale manipulation of oxygen vacancy concentration at a 24° symmetric tilt GB in SrTiO₃ by using oxidation and reduction. The thermal treatments provide contrasting GB electronic structures in reduced and oxidized SrTiO₃. The changes in Ti L_{2,3} and O K edges at the GB are consistent with deliberately induced change, i.e., tuning, of GB oxygen vacancy concentration.

This letter also underscores the advanced capabilities of aberration corrected STEM for imaging and characterizing sub-nanometer scale GB structures. This GB specific tuning approach is very general in nature and can be applied to a variety of multifunctional oxides, whereby next generation interfaces could be engineered by a combination of doping and oxidation/reduction treatments.

This work was supported by the U.S. Department of Energy, Office of Basic Energy Science (DOE-BES) under Grant No. DE-FG02-92ER45475.

- ¹N. Setter and R. Waser, *Acta Mater.* **48**, 151 (2000).
- ²Z. L. Zhang, W. Sigle, F. Phillipp, and M. Ruhle, *Science* **302**, 846 (2003).
- ³D. A. Muller, N. Nakagawa, A. Ohtomo, J. L. Grazul, and H. Y. Hwang, *Nature (London)* **430**, 657 (2004).
- ⁴A. Ohtomo, D. A. Muller, J. L. Grazul, and H. Y. Hwang, *Nature (London)* **419**, 378 (2002).
- ⁵K. D. Johnson and V. P. Dravid, *Interface Sci.* **8**, 189 (2000).
- ⁶L. M. Levinson and D. C. Hill, *Phenomena in Electroceramics* (American Ceramic Society, Columbus, OH, 1986), Vol. 1.
- ⁷R. F. Klie and N. D. Browning, *Appl. Phys. Lett.* **77**, 3737 (2000).
- ⁸R. F. Klie, M. Beleggia, Y. Zhu, J. P. Buban, and N. D. Browning, *Phys. Rev. B* **68**, 214101 (2003).
- ⁹V. Ravikumar, R. P. Rodrigues, and V. P. Dravid, *Phys. Rev. Lett.* **75**, 4063 (1995).
- ¹⁰R. A. De Souza, J. Fleig, J. Maier, O. Kienzle, Z. L. Zhang, W. Sigle, and M. Ruhle, *J. Am. Ceram. Soc.* **86**, 922 (2003).
- ¹¹R. A. De Souza, J. Fleig, J. Maier, Z. L. Zhang, W. Sigle, and M. Ruhle, *J. Appl. Phys.* **97**, 053502 (2005).
- ¹²To allow dc *I-V* characterization, four collinear Ni/Cr contact pads (1 × 3 mm²) were thermally evaporated onto the samples (10 × 10 × 0.5 mm³). Two contacts were deposited on each side of the bicrystal, running parallel to the GB. The sample geometry and electrode arrangement are shown in Fig. 1. All electrodes were equally spaced (1 mm apart). Constant dc current was supplied to the outer electrodes by a Keithley 220 Current Source, and the voltage drop across the inner electrodes was measured with a Keithley 196 Digital Multimeter (Keithley Instruments, Inc.).
- ¹³P. E. Batson, N. Dellby, and O. L. Krivanek, *Nature (London)* **418**, 617 (2002).
- ¹⁴P. D. Nellist, M. F. Chisholm, N. Dellby, O. L. Krivanek, M. F. Murfitt, Z. S. Szilagyi, A. R. Lupini, A. Borisevich, W. H. Sides, and S. J. Pennycook, *Science* **305**, 1741 (2004).
- ¹⁵S. J. Pennycook, A. R. Lupini, A. Kadavanich, J. R. McBride, S. J. Rosenthal, R. C. Puetter, A. Yahil, O. L. Krivanek, N. Dellby, P. D. L. Nellist, G. Duscher, L. G. Wang, and S. T. Pantelides, *Z. Metallkd.* **94**, 350 (2003).
- ¹⁶S. J. Pennycook and L. A. Boatner, *Nature (London)* **336**, 565 (1988).
- ¹⁷The *I-V* measurements of single crystals undergoing the same oxidation or reduction treatments are identical indicating that the bulk defect chemistry is not altered.
- ¹⁸R. D. Leapman, L. A. Grunes, and P. L. Fejes, *Phys. Rev. B* **26**, 614 (1982).
- ¹⁹V. J. Keast, A. J. Scott, R. Brydson, D. B. Williams, and J. Bruley, *J. Microsc.* **203**, 135 (2001).
- ²⁰Z. L. Zhang, W. Sigle, and M. Ruhle, *Phys. Rev. B* **66**, 094108 (2002).
- ²¹S. D. Berger, J. M. Macaulay, and L. M. Brown, *Philos. Mag. Lett.* **56**, 179 (1987).
- ²²Y. Nakano, M. Watanabe, and T. Takahashi, *J. Appl. Phys.* **70**, 1539 (1991).
- ²³V. Ravikumar, R. P. Rodrigues, and V. P. Dravid, *J. Am. Ceram. Soc.* **80**, 1117 (1997).
- ²⁴V. Ravikumar, R. P. Rodrigues, and V. P. Dravid, *J. Am. Ceram. Soc.* **80**, 1131 (1997).